The Be/X-ray Binary LSI+61^{0}303
in terms of Ejector-Propeller Model

Radoslav Zamanov[1], Josep Martí[2], and Paolo Marziani[1]

[1] Osservatorio Astronomico di Padova, Vicolo dell'Osservatorio 5, I-35122 Padova, Italy
  e-mail: `zamanov@pd.astro.it`   e-mail: `marziani@pd.astro.it`

[2] Departamento de Física, EPS, Universidad de Jaén, C/ Virgen de la Cabeza, 2, E–23071 Jaén, Spain
  e-mail: `jmarti@ujaen.es`

Abstract. We tested the ejector-propeller model of the Be/X-ray binary LSI+61^{0}303 by using the parameters predicted by the model in the calculations of the X-ray and radio variability. The results are: (1) in terms of the Ejector-Propeller model, the X-ray maximum is due to the periastron passage; (2) the radio outburst can be really a result of the transition from the propeller to the ejector regimes; (3) the radio outburst will delay with respect to the X-ray maximum every orbital period. The proposed scenario seems to be in good agreement with the observations.

Key words. stars: individual: LS I+61°303– stars: emission line, Be – radio continuum: stars – X-ray: stars

1. Flaring behaviour of LS I+61°303

LS I+61°303 (V615 Cas, GT0236+620) is a well known Be/X-ray binary with periodic radio outbursts every 26.5 d, assumed to be the orbital period. After the discovery of such periodic events (Gregory & Taylor 1978; Taylor & Gregory 1982) and the first model (Maraschi & Treves, 1981), this massive system has been studied extensively since nearly two decades ago. Hereafter, we will use the late radio phase ephemeris $P = 26.4917\,d$ and phase zero at JD2443366.775 (Gregory, Peracaula & Taylor, 1999).

The flaring radio emission of LS I+61°303 has been modeled by Paredes et al. (1991) as synchrotron radiation from an expanding plasmon containing relativistic particles and magnetic fields. The dependence of the radio outburst flux density on the frequency, the time delay in the outburst peak, and the general shape of the radio light curves are in general well accounted for by continuous injection of synchrotron emitting electrons into the plasmon volume. However, the formation details of such plasmon were beyond the scope of the Paredes et al. (1991) model. In fact, its initial physical properties were considered as the free parameters to be fitted. According to Zamanov (1995), the genesis of such plasmon can be interpreted as a result of a transition in the accretion regime of the neutron star as it probes different parts of the Be envelope in an eccentric orbit. The proposed transition would be from so called propeller (P) to the Ejector (E) regime. In this context, propeller means accretion onto the magnetosphere and ejector is often named "young radio pulsar".

Our purpose here is to try to check the agreement between the plasmon parameters predicted by the theory of a PE transition and those required to reproduce the observed radio light curves using the Paredes et al. (1991) model. We advance here that the agreement seems to be good at least qualitatively, including the possibility to explain the X-ray luminosity and variability. This agreement provides a consistent physical interpretation for the outburst mechanism in the LS I+61°303 system.

2. Simultaneous Radio and X-ray observations

The variability of the source in the X-ray domain was detected in ROSAT observations (Goldoni & Mereghetti, 1995). On two occasions, the LS I+61°303 flaring events have been monitored by ground based radio facilities and space X-ray satellites in a coordinated way. The results were presented in Taylor et al.(1996) and Harrison et al.(2000). The behavior observed is reproduced in Fig. 1, using the latest ephemeris determination. The observations during 1992 are obtained with ROSAT (0.5-2 keV) and the VLA (1.5 GHz and 4.9 GHz), and those during 1996 - with RXTE (2-10 keV) and GBI [1] (2.25 GHz and 8.3 GHz). From this figure, it is clear that in both cases the radio peak is delayed with respect to X-ray maximum.

3. Mass accretion rate

---

[1] The Green Bank Interferometer is a facility of the USA National Science Foundation operated by NRAO in support of the NASA High Energy Astrophysics programs.
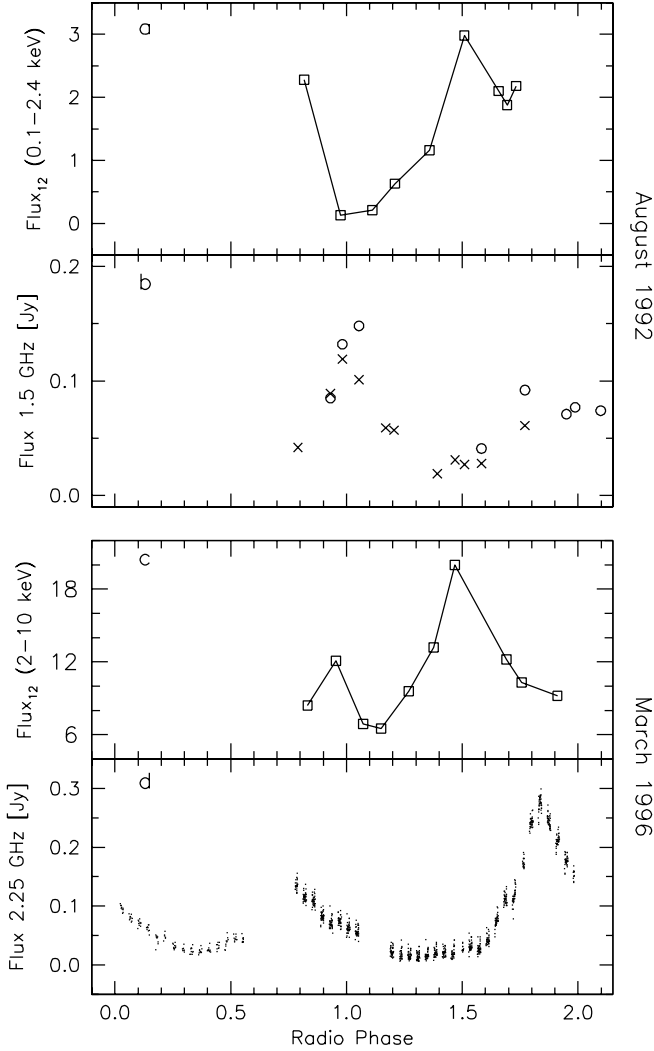
Fig. 1. The simultaneous X-ray and radio observations:
(a) and **(b)** – August 1992, Taylor et al. (1996)
(c) and **(d)** – March 1996, Harrison et al. (2000)
A clear phase shift between X-ray and radio is visible in both cases.
In **(b)** the triangles refer to 1.5 GHz and the crosses – to 4.9 GHz flux density. The X-ray flux is everywhere in units 10^{-12} erg cm^{-2} s^{-1}.

3.1. Bondi-Hoyle accretion

Usually, to estimate the mass accretion rate onto a compact object in wind fed binaries the Bondi-Hoyle-Littleton formula is used in the form:

$$\dot{M}_a = \pi \frac{(2GM_{NS})^2}{V_{rel}^3} \rho, \qquad (1)$$

where M_{NS} is the mass of the neutron star, V_{rel} is the NS velocity relative to the surrounding matter, ρ is the density in the surrounding matter.

The structure of the Be star disks are not yet well understood, even for the most important parameters, such as the ve-

locity and density laws, different assumptions have been proposed. Following Waters et al. (1988), we will accept a density structure in the form

$$\rho = \rho_0(r/R_*)^{-n} \quad \text{and} \quad V_r = V_0(r/R_*)^{n-2}, \qquad (2)$$

where R_* is the radius of the Be star and V_r is the outward velocity. The density parameter n can take values $n = 2 - 4$ for different objects. The initial velocity, V_0 (the velocity at $r = R_*$), most probably lies between 2 and 20 km s^{-1}. Finally, a Keplerian law is adopted concerning the disk rotation:

$$V_\phi(r) = \sqrt{GM_1/r} \qquad (3)$$

where M_1 is the mass of the primary component in the system, i.e. the Be star.

As a result of the motion of the neutron star throw the Be circumstellar disk the mass accretion rate will vary along the orbital period. A few examples, calculated using different parameters for the Be circumstellar disk, are shown in Fig.2. During the calculations we assumed always an orbital eccentricity $e = 0.6$, a neutron star mass of $M_{NS} = 1.4\,M_\odot$, $M_1 = 10\,M_\odot$ and an orbital period P_{orb}=26.4917 days.

As it is visible in Fig.2, we can obtain very strange mass accretion rates in some cases. In Fig.2(b,c), the average mass accretion rate is considerably higher than the mass loss rate of the Be star. This is a false result of the used formula. The Bondi-Hoyle description is valid for accretion from infinite medium. It assumes that all the matter entering into a cylinder with radius equal to the accretion radius ($R_a = \sqrt{2GM_{NS}/V_{rel}^2}$) will be accreted. In the context of a binary star, this is only valid provided that

- the motion is high supersonic $V_{rel} >> C_s$,
- $R_a << r$,
- the whole accretion cylinder is filled with the outflowing wind.

Unfortunately these conditions are not always fulfilled in Be/X-ray binary systems.

## 3.2. Mass accretion rate in Be/X-ray binaries

As it was shown in the previous section the Bondi-Hoyle formulae are not giving good results in case of Be/X-ray binaries. The exact mass accretion rate could be found only if we consider simultaneously the formation of the wind and the influence of the compact object onto the wind. Here we propose a modification of the mass accretion rate formula that is appropriate for Be/X-ray binaries. In order to do so, the Bondi-Hoyle formula has to be rewritten in a way such that the accretion radius explicitly appears:

$$\dot{M}_a = \pi R_a^2\, \rho\, V_{rel}\,, \qquad (4)$$

where the density in an outflowing wind, with disk opening angle θ, is given from the continuity equation:

$$\dot{M}_{loss} = 4\pi r^2 \sin\theta\, V_w\, \rho, \qquad (5)$$

The wind in the disk is most probably subsonic (i.e. Okazaki, 2001). A keplerian rotation in the disk will give in
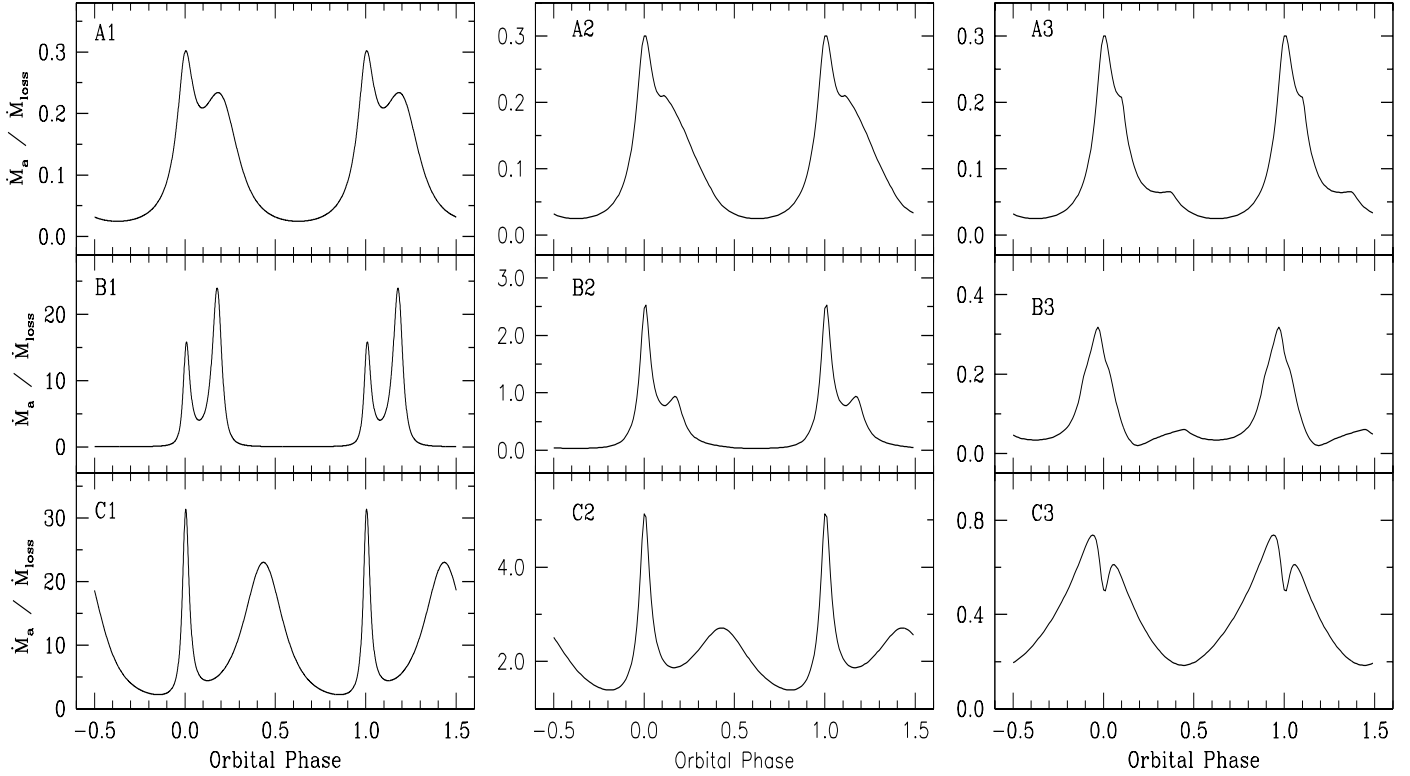
Fig. 2. Mass accretion rate using the Bondi-Hoyle formulae. Everywhere the orbital parameters are $M_1 = 10\,M_\odot$, $M_{NS} = 1.4\,M_\odot$, P_{orb}=26.4917 d, $e = 0.6$. The wind parameters used and the calculated average mass accretion rate are :

(A1) V_0=5 km s^{-1}, $n = 3.25$, non-rotating disk, $\overline{\dot{M}_a} = 0.11\,\dot{M}_{loss}$

(B1) V_0=5 km s^{-1}, $n = 3.25$, keplerian disk, $\overline{\dot{M}_a} = 2.9\,\dot{M}_{loss}$

(C1) V_0=10 km s^{-1}, $n = 2.1$, keplerian disk, $\overline{\dot{M}_a} = 9.7\,\dot{M}_{loss}$

The use of the Bondi-Hoyle formula gives obviously false values(at least in A1 and B1) values of the average mass accretion rate:

(A2), (B2), (C2) - the same parameters, but the factor of the filling of the accretion cylinder included.

(A3), (B3), (C3) - the same parameters, but the upper limit set $R_a \leq r/4$, and the filling factor included. The corresponding average mass accretion rates are $\overline{\dot{M}_a}/\dot{M}_{loss} = 0.09, 0.08, 0.36$, for A3, B3, and C3 respectively.

many cases a low relative velocity between the NS and the wind. This means that the accretion radius depends also on the speed of sound, c_s :

$$R_a = \frac{2GM_{NS}}{V_{rel}^2 + c_s^2} \qquad (6)$$

Using this formula (with or without C_s^2 term), the accretion radius of a neutron star can achieve values bigger than the distance between components. However the disks in the Be/X-ray binaries are more or less similar to the disks in the "normal" Be stars (Zamanov et al. 2001) although some differences exist. This means that the accretion radius can not be very big, otherwise the NS would control the motion of the wind and this is impossible because the mass ratio is $M_1/M_{NS} > 4$ (typically $M_1 > 8\,M_\odot$ and $M_{NS} = 1.4 M_\odot$) We will thus adopt here

an upper limit $R_a < 0.25\,r$, where r is the distance from the Be star

Because the outflowing wind is confined in a disk, it is possible that the vertical size of the disk is less than the accretion radius. Consequently, the accretion cylinder would not entirely filled by the wind material. In case that $R_a > y$ where y is the vertical size of the outflowing disk $y = r\sin\theta$, the accretion rate must be reduced with pure geometrical factor $2\pi R_a^{-2}[y\sqrt{R_a^2 - y^2} + R_a^2 \sin^{-1}(y/R_a)]$.

We believe that the proposed modifications give considerably better results concerning the mass accretion rate, i.e. the NS will accrete a fraction of the wind. The results of the calculations are demonstrated in Fig.2 A3,B3,C3.
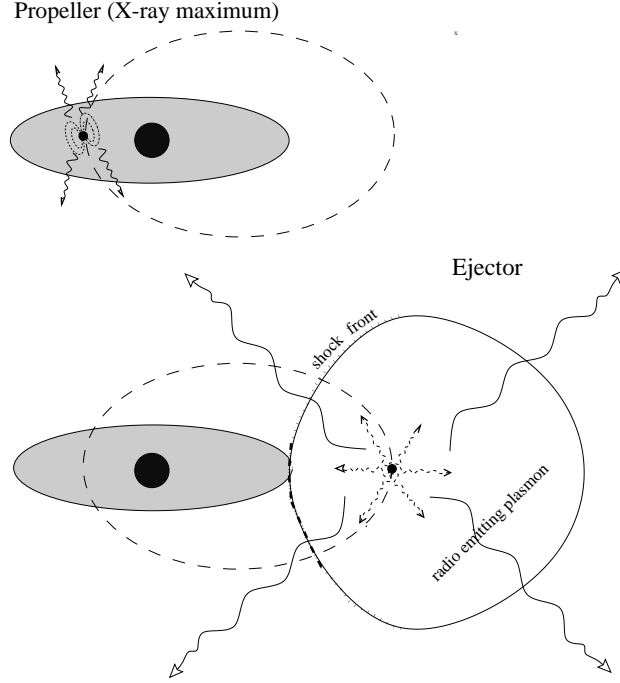
Fig. 3. A sketch of the Ejector-propeller model. The dashed lines indicates the orbit of the neutron star. Upper - accretion onto the magnetosphere at periastron, down - ejector and the cavern around the neutron star.

4. X-ray variability in the light of Ejector-Propeller model

A sketch of the ejector-propeller model of LS I+61°303 is illustrated in Fig.3. Following the suppositions the neutron star will act as propeller (accretion onto the magnetosphere) at periastron and as ejector (young radio pulsar) at the apastron. The transitions between the regimes will depend how material is captured in the the neutron star accretion cylinder, possible formation of accretion disk during the accretion onto the magnetosphere, and even the possible flip-flop instability of accretion (Livio et al 1991).

Following the assumptions of the ejector-propeller model, a lower mass capture rate is expected during the ejector regime. In contrast, higher mass capture rates are expected during the propeller regime close to periastron passage. During the propeller stage the X-ray luminosity can be estimated as

$$L_X(P) = 2^{2/7}(GM)^{8/7}\mu^{-4/7}\dot{M}_a^{9/7}, \tag{7}$$

where G is the constant of gravitation, M is the mass of the neutron star, μ is its magnetic dipole moment (which is adopted $\mu = 2 \times 10^{30}$G cm³), and $\dot{M}_a$ is the mass accretion rate.

During the ejector stage efficiency of conversion of the spin-down energy into high energy emission can be expected to be about 1-10% (Tavani et al. 1996). The estimated spin-down luminosity of the ejector is expected about $1 - 5 \times 10^{35}$ erg s⁻¹, so as reasonable value can be adopted $L_X(E) = 2.10^{33} - 2.10^{34}$ erg s⁻¹.

The other possibility to estimate the X-ray luminosity of the expanding plasmon is to consider Bremsstrahlung emission of the shocked gas. In this case Taylor et al. (1996) also obtained 2×10^{34} erg s⁻¹. The both estimates are in good agreement

and are similar to the expected values of the magnetospheric accretion.

It deserves to be noted that in case of transition between accretor and propeller a considerable luminosity gap will exist, about 100 times difference in the X-ray luminosity, is expected and observed (Corbet 1996; Raguzova & Lipunov, 1998). But this is not the case at the transition between ejector and propeller, where the X-ray luminosities are of the same order. So, we will assume that $L_X(ejector) = L_X(propeller)$ not to complicate our qualitative results.

The X-ray luminosity calculated in this way is plotted in Fig.4. The orbital phase zero corresponds to the periastron, the adopted mass loss rate of the Be star is $M_{loss} = 10^{-9} M_\odot$ yr⁻¹. The calculated X-ray variability is very similar to the observed (Fig. 1). The X-ray maximum is at periastron and this means that the periastron passage corresponds to radio phase ~ 0.5 using the modern radio ephemeris.

5. Plasmon parameters and radio outbursts

The switch on of the ejector will create a cavern around the neutron star. This cavern will start to expand under the pressure of the relativistic wind of the ejector and can be identified with the expanding plasmon, which radio emission successfully fit the observed radio outbursts of LS I+61°303 modeled by Paredes et al. (1991). The question here is: are the parameters expected at the propeller-ejector transition appropriate for the plasmon?

The most important parameters which appeared in the radio model of Paredes et al. (1991) are initial radius (R_0), expansion velocity ($V_{\exp}$), initial magnetic field, injection time interval, power law index of electrons, and the injection rate. In
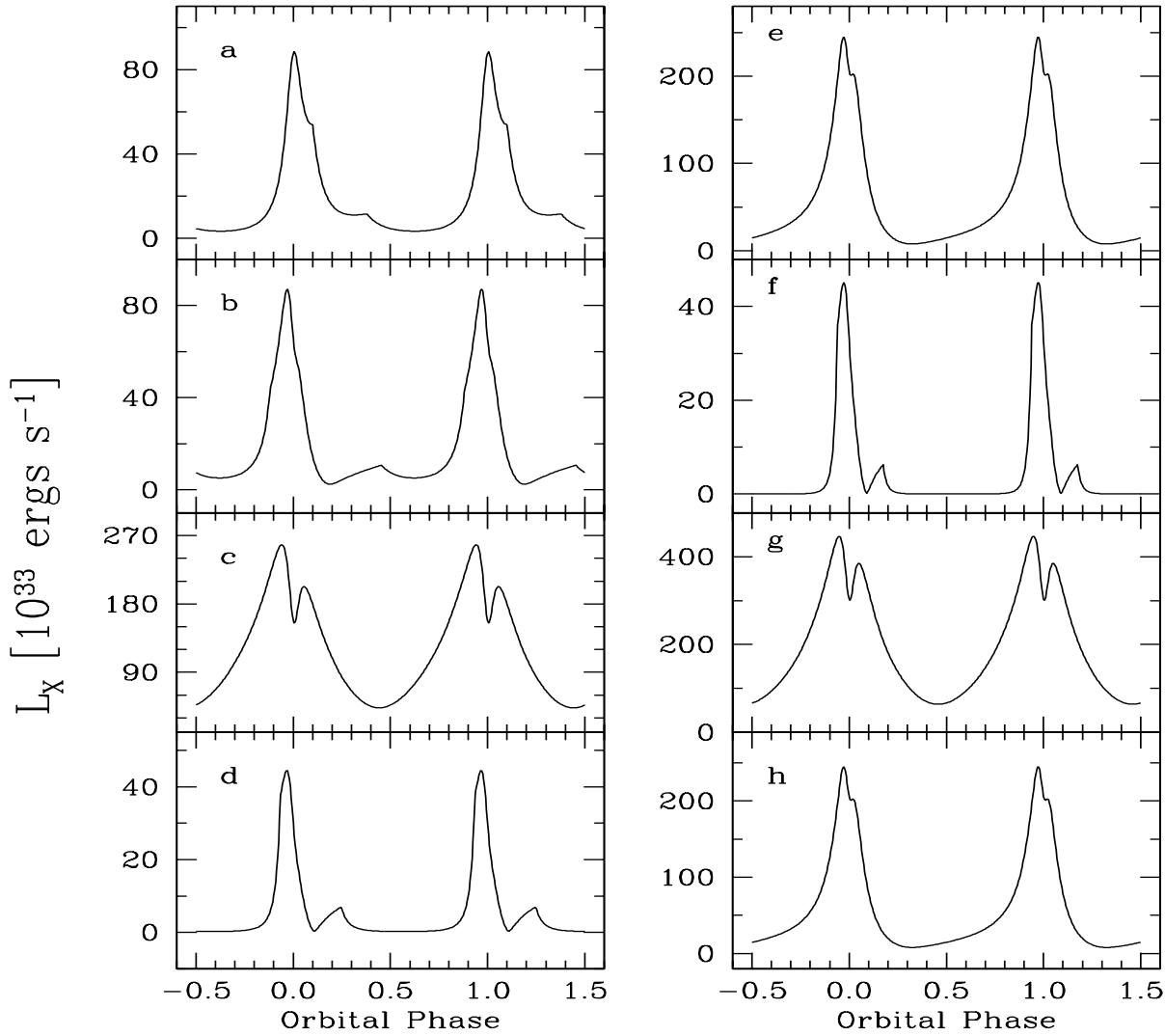
Fig. 4. The calculated X-ray luminosity of the the neutron star in LS I+61°303 using different wind parameters. The L_X is calculated as magnetospheric accretion luminosity and supposing that $L_X(ejector) = L_X(propeller)$. The radio outbursts are expected to peak after the X-ray maximum, when the mass accretion rate is lower, and the NS can change its regime from propeller to ejector.

(a) V_0=5 km s^{-1}, $n = 3.25$, non-rotating disk, $\overline{\dot{M}_a} = 0.09 \, \dot{M}_{loss}$

(b) V_0=5 km s^{-1}, $n = 3.25$, keplerian disk, $\overline{\dot{M}_a} = 0.08 \, \dot{M}_{loss}$

(c) V_0=10 km s^{-1}, $n = 2.1$, keplerian, $\overline{\dot{M}_a} = 0.36 \, \dot{M}_{loss}$

(d) V_0=10 km s^{-1}, $n = 3.25$, keplerian, $\overline{\dot{M}_a} = 0.03 \, \dot{M}_{loss}$

(e) V_0=2 km s^{-1}, $n = 3.25$, keplerian, $\overline{\dot{M}_a} = 0.20 \, \dot{M}_{loss}$

(f) V_0=5 km s^{-1}, $n = 3.75$, keplerian, $\overline{\dot{M}_a} = 0.02 \, \dot{M}_{loss}$

(g) V_0=5 km s^{-1}, $n = 2.25$, keplerian, $\overline{\dot{M}_a} = 0.53 \, \dot{M}_{loss}$

(h) V_0=2 km s^{-1}, $n = 3.25$, keplerian, $\overline{\dot{M}_a} = 0.20 \, \dot{M}_{loss}$

Everywhere we adopted mass loss rate in the outflowing disk $M_{loss} = 10^{-9} \, M_\odot \, yr^{-1}$.

the terms of Ejector-propeller model we can put constrains on the allowed ranges for this parameters:

- 1. The time of plasmon appearance - the plasmon will appear after the periastron passage at low mass accretion rate (for more details see Zamanov, 1995 and references therein). So it means that the radio outbursts will peak always with some phase shift after the change of the regime from propeller to ejector.

- 2. The initial radius expected at the propeller-ejector transition will be of the order of light cylinder radius, and in any case less than the accretion radius, which means that acceptable values are of the order of $0.01 - 3.0 \, R_\odot$

- 3. The expansion velocity of the cavern in terms of the propeller-ejector transition can be estimated as (Zamanov, 1995):

$$V_{\exp} = V_{\mathrm{w}} + \sqrt{L_m V_w/(c\dot{M}_{loss})} \qquad (8)$$

where c is the speed of light, $\dot{M}_{loss}$ and V_w are the mass loss rate and the wind velocity of the Be star respectively, L_m is magneto-dipole luminosity of the young radio pulsar. Adopting $V_w = 100\,\mathrm{km\,s^{-1}}$ for the disk wind and $V_w = 1000\,\mathrm{km\,s^{-1}}$ for the polar wind and $L_m = 1-5\times10^{35}\mathrm{erg\,s^{-1}}$ the cavern expansion will be with velocity $200 - 1300\,\mathrm{km\,s^{-1}}$. In the radio light curves we will adopt values $V_{\exp}$ =200, 400, 1200 km s^{-1}.

- 4. Injection time interval - it is the time neutron star acts as ejector. The switch on of the ejector will be when the neutron star goes away from the B star and the switch off will be when it enters in the dense circumstellar disk approaching the periastron. From the mass accretion rate behavior (Fig.2 right and Fig.4) we can expect injection time interval $0.4 - 0.7 \times P_{orb}$ or in other words $10 - 20$ days.

- 5. Injection rate - the total injection rate of the Crab into the nebula at a spin period of 0.033 s^{-1} is estimated to be about 10^{40}-10^{41} particles s^{-1} on base of the high-energy spectrum (De Jager & Harding, 1992). From one side the spin period of the neutron star in LS I+61°303 required from the E-P model is longer than Crab. We expect $P_{spin} = 0.15 - 0.20\,s$ (see Zamanov 1995 for more details). It means $\sim 100 - 1000$ times lower rate of injected relativistic particles ($L_m \sim P_{spin}^{-4}$). From other side as a result of the magnetosphere accretion there are probably more particles for injection. We will adopt $5\times10^{-38}\,e^-\,\mathrm{s^{-1}}$

- 6. Magnetic field - the origin of magnetic field inside the plasmon will be something like to the magnetic field of the Crab nebula but some additional contribution from the B star is possible. The magnetic field referred in the "radio" figures (Fig.5) are very high because they refer to the magnetic field at the initial plasmon radius. When the plasmon expands to sizes of 1 AU, as measured with VLBI, the magnetic field is then close to 1 Gauss in agreement with VLBI estimates based on equipartition arguments. (Note: Changes in the radius and the magnetic field do no alter the light curves provided that $B\,R^2$ is constant - magnetic flux conservation).

- 7. Electron power law index is adopted $p = 1.6$, in order to be consistent with observed non-thermal (i.e. negative) spectral indices when the plasmon becomes optically thin. According to synchrotron theory, the optically thin spectral index is $\alpha = (1 - p)/2$. In our case, we have then $\alpha = -0.3$ in agreement with typical observations.

- 8. Energy range of relativistic electrons:
$m_e c^2 < E < 10^{-2}\,erg$

- 9. Distance from the Earth: 2 kpc

Using the above parameters appropriate for the ejector-propeller model and the plasmon prescription we generated radio light curves. They are shown in Fig.5. The radio behavior (amplitude and shape) is very similar to the observed in the radio monitoring of LS I+61°303.

6. Discussion

Using the parameters appropriate to the ejector-propeller model we calculated the X-ray and radio variability of the Be/X-ray binary LS I+61°303. The general shape of the radio behavior (amplitude and shape) is very similar to the observed in the radio monitoring of LS I+61°303, as it was already shown in the "plasmon" calculations by Paredes et al.(1991). The radio outbursts peak can be achieved 2-8 days after the appearance of the plasmon (see Fig.5). The appearance of the plasmon can be expected when the neutron star emerges from the denser part of the disk, i.e. $2-5$ days after the periastron (orbital period is 26.5 days). In the calculated X-ray curves the X-ray maximum corresponds to the periastron. The switch on of the ejector will be $0.1 - 0.4\,P_{orb}$ later. It means that the radio peak will delay with 3-13 days after the X-ray maximum. This is the behavior observed in both cases of the simultaneous radio and X-ray observations (Fig.1). As can be seen in Fig.4, the total X-ray luminosity expected in Ejector-Propeller model is of the order $1 - 200 \times 10^{33}$ erg s^{-1} This is in good agreement with the observed by ASCA (Paredes et al. 1997) variability $1 - 6 \times 10^{34}$ erg s^{-1} in the 2-10 keV band.

6.1. High resolution radio maps

Recent high resolution radio maps have evidenced a one sided radio jet at milliarcsecond scales (Massi et al. 2001). These authors interpret it as a microquasar bipolar ejection with significant Doppler boosting effect. The ejector-propeller model, explored in this paper, provides however an alternative interpretation. Considering that the plasmon will be formed in one side of the Be star (the apastron vicinity), a one sided radio jet is naturally expected.

6.2. Asymmetry of the cavern

To model the radio light curves we assumed that the plasmon expansion is spherically symmetric. But in the real case this region will be not symmetric. Different forms of the cavern are possible - closed or open, for more details see Lipunov & Prokhorov (1984). In addition, the fact that the neutron star ejects relativistic particles at the apastron of an eccentric orbit will lead to a radio source which is elongated in the direction of apastron. In any case, the radio source formed around the ejecting neutron star will be elongated in the direction controversial to the direction to the B star.

6.3. Strong and weak radio outbursts

It was discovered that radio outburst peak flux density varies over a time scale of 1600 days. On the same time scale the $H\alpha$ emission of the outflowing disk (Zamanov & Marti, 2000) varies as well, and may be even the X-ray maximum (Apparao 2001). Our preliminary tests evidenced that a slower expansion velocity and stronger magnetic field give higher radio peak flux densities and the outburst peaks later. Also a faster expansion velocity and lower magnetic field will result into lower peak flux densities and the earlier outburst peaks. These effects and

their connection with the conditions in the Be disk need of careful modeling.

6.4. Multiple Outbursts

A mechanism of multiple formation of caverns around an ejecting neutron star is proposed (Lipunov & Prokhorov, 1983). We can speculate that, in case of multiple peaks in the LS I+61°303 radio outbursts, we may be observing such a multiple cavern formation. Another possibility is a density structure in the wind of the Be star, i.e. rings with higher density that can change the regime more than once during an orbital period.

6.5. Gamma rays

During the Ejector stage the gamma ray emission is thought to originate in the shock front at the boundary of the pulsar and stellar winds (Kniffen et al. 1997). Gamma ray production is possible during the propeller action too. Possible mechanisms are double layer formation in the interblob plasma (Wynn, King & Horne, 1997) or high voltage at the boundaries of vortex structures (Wang and Robertson, 1985).

6.6. Other possibilities

The fact that the radio outbursts are not exactly periodical point to they are a result of a process which has appropriate conditions to begin somewhere at radio phases 0.5-1.0, but when the process will switch on is a by-chance. We suppose that this process is the transition of the neutron star from propeller to ejector. Another alternative is the transition closed-open cavern around the ejecting neutron star (Zamanov 1995b, Harrison et al. 2000). In this case the expected magneto-dipole luminosity of the neutron star is about 6×10^{36} erg s^{-1}, i.e. 10 times more than the expected in the ejector-propeller model.

It can not be excluded that a magnetized black hole is acting in LS I+61°303 (Punsly, 1999). If such a compact object does exist in LS I+61°303, the microquasar scenario proposed by Massi et al. (2001) should be also considered seriously. Further observations are required in order to finally solve the true nature of this X-ray binary.

7. Conclusions

We tested the ejector-propeller model for the radio-emitting Be/X-ray binary LS I+61°303. The calculations show that the X-ray variability and radio outbursts can be the result of the transition from the propeller to the ejector accretion regimes every orbital period. The main results are:

- The parameters expected from the ejector-propeller model are appropriate for the radio plasmon and the calculated radio light curves are similar to the observed radio outbursts in LS I+61°303.

- In terms of Ejector-Propeller model the X-ray maximum is a result of the propeller action during the periastron passage of the neutron star.

- The periastron is expected to correspond with radio phase ~ 0.5 using the late radio ephemeris - i.e. the time of the X-ray maximum.

- The observed phase shift between the radio and the X-ray maxima is in agreement with the ejector-propeller model of LS I+61°303. We expect that the X-ray and the radio maxima will always peak at different orbital phase.

- The total X-ray luminosity expected in terms of Ejector-Propeller model $1 - 200 \times 10^{33}$ erg s^{-1} is in good agreement with the observed by ASCA (Paredes et al. 1997) variability $1 - 6 \times 10^{34}$ erg s^{-1} in the 2-10 keV band.

There are a few systems where it is expected that the neutron star survives transitions from propeller to accretor and backward - A 0538-66, X 0331+53 (Raguzova & Lipunov, 1998). In our opinion, LS I+61°303 is probably the first example where we observe the transition from ejector to propeller and backward to occur every orbital period.

During the lives of neutron stars in binary systems, it is believed that they evolve through different stages - ejector, propeller, accretor (Lipunov et al. 1994). Studies over systems such as LS I+61°303, A 0538-66 and X 0331+53, which probably exhibit transitions between these different regimes, will give us the unique possibility to investigate these transitions over a time scale of months. This is an interval of time extremely short considering that the transitions, which are result of the neutron star evolution, occur on much longer time scales (~ 10 Myr). New light over the evolution of the neutron stars in binary systems is expected from this kind of work.
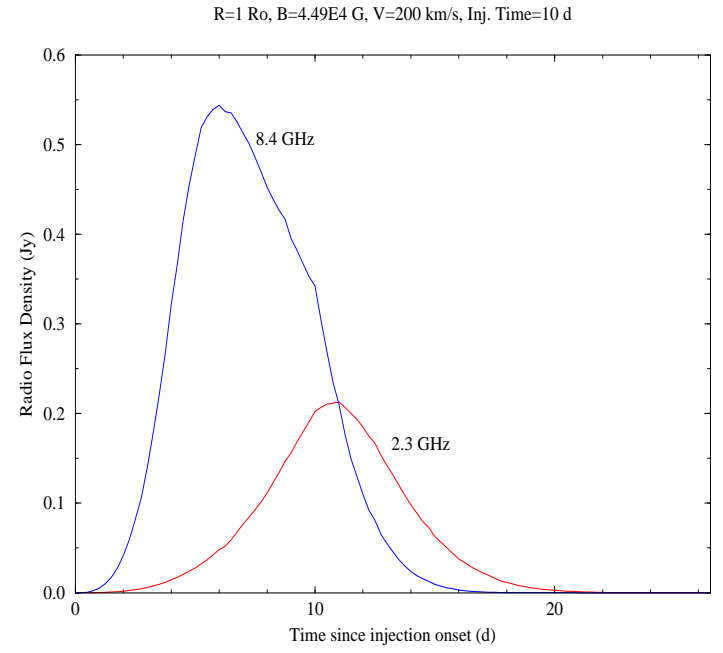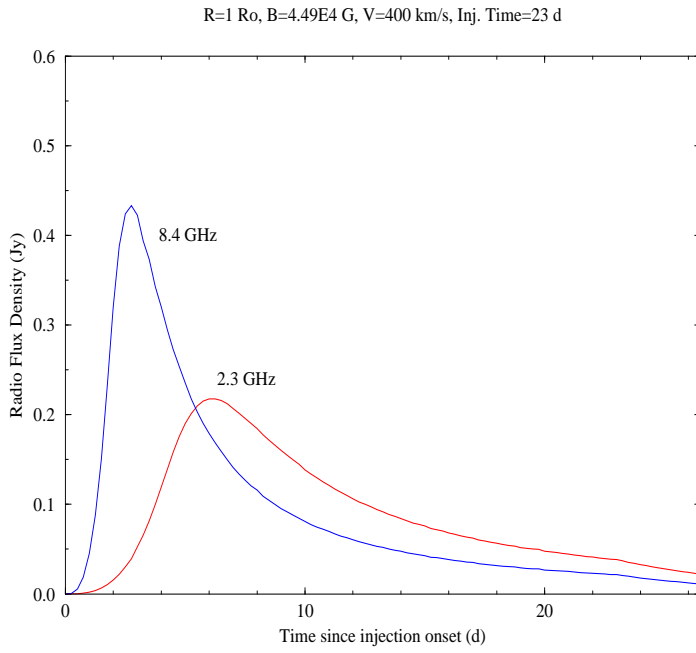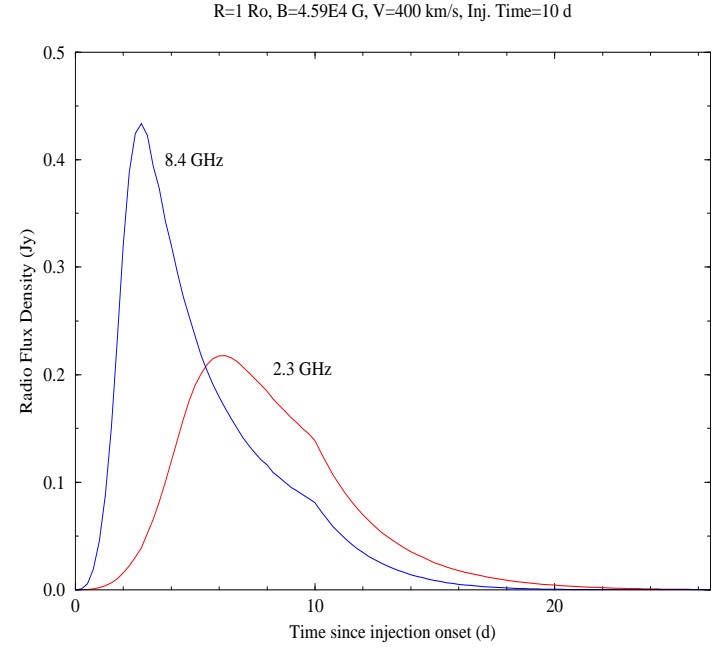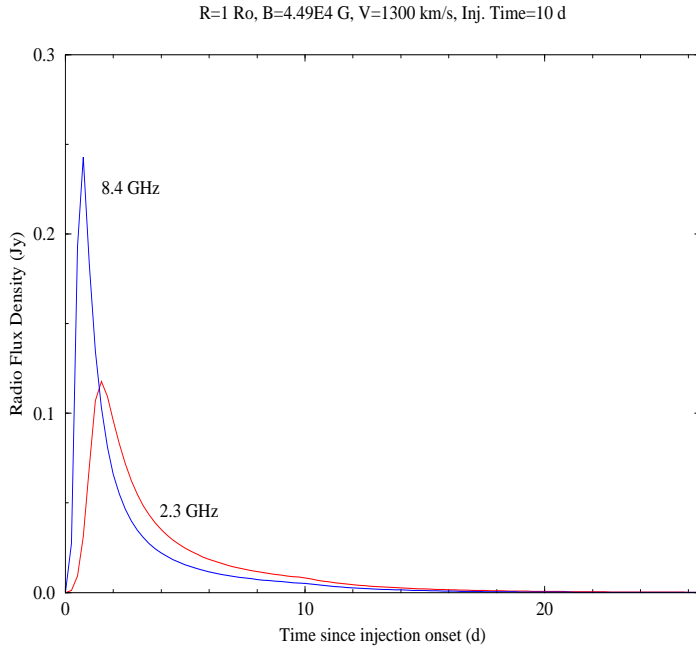
References

Apparao K.M.V., 2001, A&A 371, 672
Corbet R.H.D., 1996, ApJ 457, p.L31
De Jager O.C., Harding A.K., 1992, ApJ 396, 161
Goldoni P., Mereghetti S., 1995, A&A 299, 751
Gregory P.C., Peracaula M., Taylor A.R., 1999, ApJ 520, 376
Gregory P.C. & Taylor A.R., 1978, Nature 272, 704
Hutchings J.B., Crampton D., 1981, PASP 93, 486
Harrison F.A., Ray P.S., Leahy D.A., Waltman E.B., Pooley G.G., 2000, ApJ 528, 454
Daugherty J.K. & Harding A.K., 1982, ApJ 252, 337
Kniffen D., Alberts W.C.K, Bertsch D.L., et al., 1997, ApJ 486, 126
Lipunov V.M., Prokhorov M.E., 1984, Ap&SS 98, 221
Lipunov V.M., Nazin S.N., Osminkin E.Yu., Prokhorov M.E., 1994, A&A 282, 61
Livio M., Soker N., Matsuda T., Anzer U., 1991, MNRAS 253, 633
Maraschi L. & Treves A., 1981, MNRAS 194, 1p
Massi M., Ribo M., Paredes J., Peracaula M., Estalella R., 2001, A&A, 376, 217
Mendelson H., Mazeh T., 1994, MNRAS 267, 1
Okazaki A.T., 2001, PASJ 53, 119
Paredes J.M., Martí J., Estalella R., Sarrate J., 1991, A&A 248, 124
Paredes J.M., Martí J., Peracaula M., Ribó M., 1997, A&A 320, L25
Punsly B., 1999, ApJ 519, 336
Raguzova N.V., Lipunov V.M., 1998, A&A 340, 85
Tavani M., Hermsen W., van Dijk, R. Strickman M., Zhang S.N., Foster R.S., Ray P.S., Mattox J., Ulmer M., Purcell W., Coe M., 1996, A&AS 120C, 243

Waters L.B.F.M., Taylor A.R., van den Heuvel E.P.J., Habets
    G.M.H.J., Persi P., 1988, A&A 198, 200
Wang Y.-M., Robertson J.A., 1985, A&A 151, 361
Wynn G.A., King A.R., Horne K., 1995, MNRAS 286, 436
Zamanov R.K., 1995a, MNRAS 272, 308
Zamanov R.K., 1995b, Comp.Rend.Acad.bulg.Sci. 48, N: 5, 5
Zamanov R.K., Reig P., Marti J., Coe M.J., Fabregat J., Tomov T.,
    Valchev T., 2001, A&A 367, 884

Fig. 5. Radio Light curves generated using the expanding plasmon and setting parameters appropriate for the ejector-propeller model.
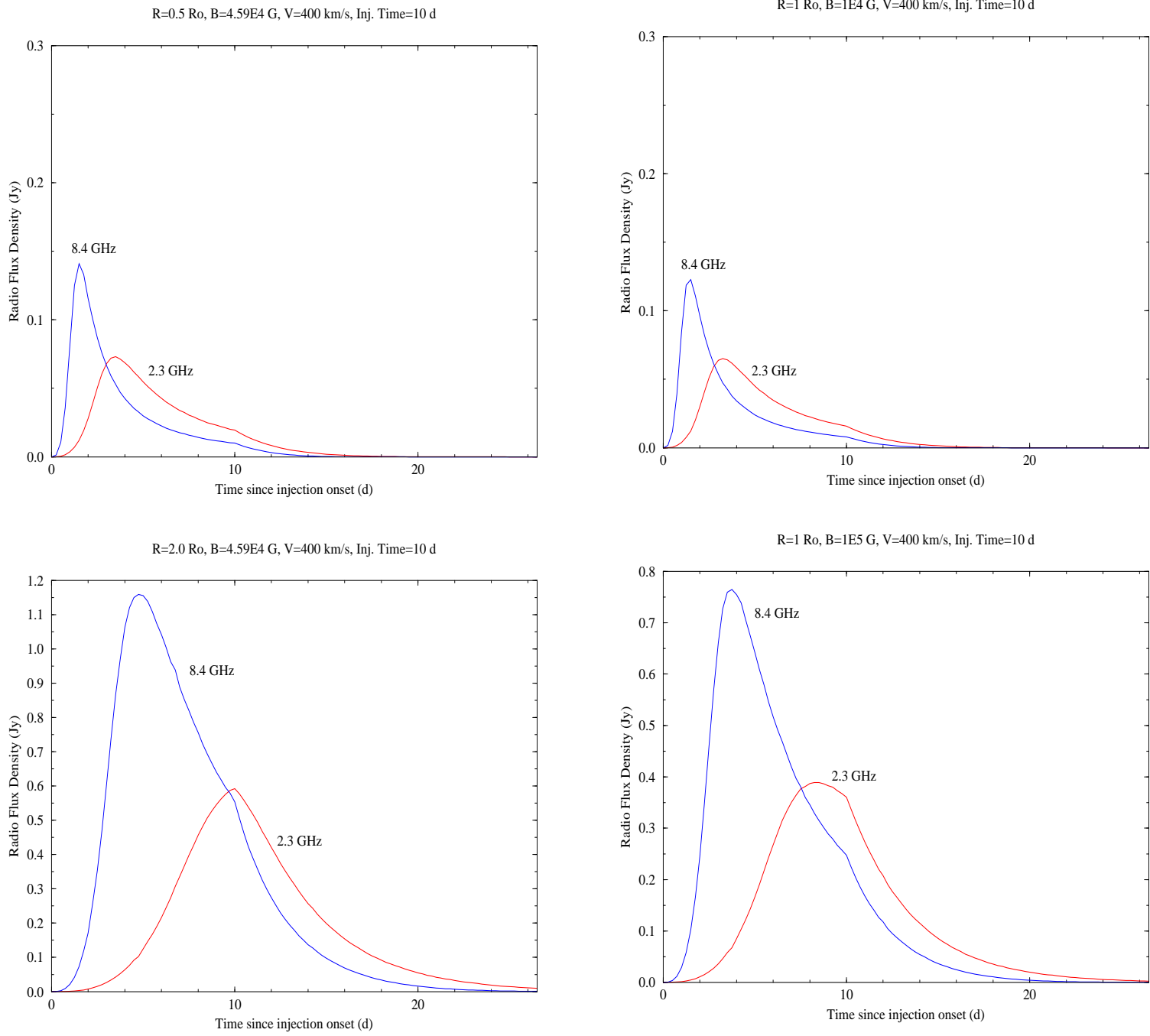
Fig. 5. continued

R=0.5 Ro, B=4.59E4 G, V=400 km/s, Inj. Time=10 d

R=1 Ro, B=1E4 G, V=400 km/s, Inj. Time=10 d

R=2.0 Ro, B=4.59E4 G, V=400 km/s, Inj. Time=10 d

R=1 Ro, B=1E5 G, V=400 km/s, Inj. Time=10 d